GMSK Modulation for Deep Space Applications

Shervin Shambayati
Jet Propulsion Laboratory
California Institute of Technology
4800 Oak Grove Dr.
Pasadena, CA 91109
(818)354-1280
shervin.shambayati@jpl.nasa.gov

Dennis K. Lee
Jet Propulsion Laboratory
California Institute of Technology
4800 Oak Grove Dr.
Pasadena, CA 91109
(818)354-6908
Dennis.K.Lee@jpl.nasa.gov

Abstract*—Due to scarcity of spectrum at 8.42 GHz deep space X-band allocation, many deep space missions are now considering the use of higher order modulation schemes instead of the traditional binary phase shift keying (BPSK). One such scheme is pre-coded Gaussian minimum shift keying (GMSK). GMSK is an excellent candidate for deep space missions. GMSK is a constant envelope, bandwidth efficien modulation whose frame error rate (FER) performance with perfect carrier tracking and proper receiver structure is nearly identical to that of BPSK. There are several issues that need to be addressed with GMSK however. Specificall , we are interested in the combined effects of spectrum limitations and receiver structure on the coded performance of the X-band link using GMSK. The receivers that are typically used for GMSK demodulations are variations on offset quadrature phase shift keying (OQPSK) receivers. In this paper we consider three receivers: the standard DSN OQPSK receiver, DSN OQPSK receiver with filte ed input, and an optimum OQPSK receiver with filte ed input. For the DSN OQPSK receiver we show experimental results with (8920, 1/2), (8920, 1/3) and (8920, 1/6) turbo codes in terms of their error rate performance. We also consider the tracking performance of this receiver as a function of data rate, channel code and the carrier loop signal-to-noise ratio (SNR). For the other two receivers we derive theoretical results that will show that for a given loop bandwidth, a receiver structure, and a channel code, there is a lower data rate limit on the GMSK below which a higher SNR than what is required to achieve the required FER on the link is needed. These limits stem from the minimum loop signal-to-noise ratio requirements on the receivers for achieving lock. As a result of this, for a given channel code and a given FER, there could be a gap between the maximum data rate that BPSK can support without violating the spectrum limits and the minimum data rate that GMSK can support with the required FER depending on the type of GMSK receiver that is used.

TABLE OF CONTENTS

1. INTRODUCTION

Due to limitations on the X-band spectrum allocation for deep-space missions, many deep-space science missions are switching to Ka-band for their primary science data return. However, all these missions still have to carry an X-band system for emergency mode operations. The X-band amplifie for emergency communications needs to be rather powerful (∼60 W); therefore, absent spectrum limitations, it can support relatively high data rates over a reasonably sized antenna (∼2 m). Given this, it is of interest to evaluate the performance of X-band with bandwidth efficien modulations and to calculate the data rates it can support subject to coding, receiver, and spectrum limitations. The combination of these limitations creates a data rate profil as a function of received P_t/N_0 (total power-to-noise ratio).

Gaussian Minimum Shift Keying (GMSK) [1] is an excellent candidate as bandwidth efficien form of modulation. Using "pre-coding," the performance of GMSK with a Gaussian fil ter 3-dB bandwidth-binary symbol period product (BT) of 0.5 is nearly identical to that of binary phase shift keying (BPSK) provided that both have perfect carrier tracking [4]. Carrier tracking is part of the receiver's functions; therefore the structure of the receiver used for tracking GMSK could substantially affect its performance vis-a-vis BPSK's. In NASA's Deep Space Network (DSN), GMSK is treated as a pulse-shaped offset quadrature phase shift keying (OQPSK) with receivers designed for OQPSK modifie accordingly. This modificatio typically involves adding appropriate matched filter (MFs) based on Laurent's decomposition [2] [4] of GMSK to the standard OQPSK receivers. Absent such modifications standard OQPSK receivers could still be used for GMSK demodulation albeit with some losses.

The problem that arises with this approach is that the design of these receivers are based on the assumption that OQPSK or GMSK will be used only at relatively high data rates with relatively high rate channel codes. Unfortunately, we contend this is not a valid assumption for GMSK. The problem is as follows. Most missions are greedy in that they want to maximize their data return by using the most power-efficien combination of coding and modulation available to them. Absent of receiver or spectrum limitation, their preference is, therefore, for BPSK modulation with the channel code with the lowest E_b/N_0 that meets their data quality requirement (usually expressed in terms of either the frame or the bit error rate). However, because of spectrum limitations on X-band, as the data rate increases, a given modulation needs to switch to a higher rate channel code. This process of switching to higher channel codes will continue until either the data rate is such that even with the highest rate code available, the modulation cannot support the required data rate or a more spectrum efficien form of modulation with a lower rate code that does not violate the spectrum limits becomes more power efficien than the performance of the code that is allowed to be used with the less spectrum efficien modulation. (Note that here it is assumed that lower rate codes have better performance than higher rate codes for a given error rate.) As a rule of thumb, it is usually assumed that more spectrum efficien forms of modulation are less power-efficien and therefore, at lower data rates they cannot compete with the

978-1-4577-0557-1/12/$26.00 ©2012 IEEE.
[1] IEEEAC Paper #1639, Final Version 1.0, Updated 29/11/2011.

less spectrum-efficien modulations such as BPSK even with better lower rate channel codes. However, this is not the case with GMSK. As said before, GMSK's performance with perfect carrier tracking is almost identical to BPSK [4]. Therefore, even at lower data rates, if perfect carrier tracking is available for both BPSK and GMSK, GMSK is superior to BPSK if it can be used with a lower rate code than BPSK because of its higher spectrum efficien y. The superiority of GMSK under these conditions hinges on the ability of the receiver to track the carrier perfectly. As we will show below, how well the carrier could be tracked at lower data rates depends on the receiver design and that some of the existing and proposed designs for GMSK tracking do rather poorly. To illustrate fully, we derive the supportable data rate profil for each receiver as a function of P_t/N_0 for a given set of available channel codes and the spectrum limitations imposed on X-band for both deep space missions at Mars and non-Mars deep space missions. We then compare this performance to that of the BPSK. We will also provide experimental data for three turbo codes from tracking of GMSK signals with the existing DSN Block V Receiver (BVR) configure to track OQPSK. Note that the approach we are taking is from the spacecraft point of view, i.e., we do not consider such things as implementation complexity and cost of the ground receivers. For a real system tradeoff, such costs and complexity must be weighed against the cost in terms of data return and additional power on the spacecraft that are planning to use GMSK.

The paper is organized as follows. In Section 2 assumptions and methodology used in this paper are presented. In Section 3, the results are discussed. In Section 4, caveats and conclusions are reached.

2. Assumptions and Methodology

E_b/N_0 Operating Point for Different Channel Codes

The channel codes that are considered in this paper are (8920,1/6), (8920,1/4), (8920,1/3) and (8920,1/2) turbo codes as well as rate 2/3 and rate 4/5, block length 4096 low-density parity check (LDPC) codes and a Reed-Solomon (255, 223) code with interleaving depth of 5.

The information E_b/N_0 for each code is selected such that a block of 8920 information bits would have an error rate of 10^{-4}. This is the frame error rate (FER) that is assumed for turbo and RS codes. For LDPC codes, we use the approximation

$$10^{-4} = 1 - (1 - p_{LDPC})^{\frac{8920}{4096}} \quad (1)$$

where p_{LDPC} is the LDPC FER. In this case $p_{LDPC} = 4.59 \cdot 10^{-5}$. The corresponding information E_b/N_0 and symbol E_s/N_0 (evaluated at the output of the encoder) values for each code are presented in Table.1[2] We assume that these values are the same (excepting radio losses, see below) for all the modulations considered in this paper.

Spectrum Limitations on Different Modulation Techniques.

The spectral efficien y (or lack thereof) of a modulation scheme sets limits on the maximum bit rate (define at the input of the modulator) that could be transmitted. These limits at Mars are different from those at other parts of deep space because a relatively large number of missions operate at Mars. The data rate limitations for various codes for Mars and non-Mars missions are given in Tables 2 & 3, respectively.[3] The data rate limits presented in these tables are based on Space Frequency Coordination Group (SFCG) recommendation SFCG 23-1. This recommendation define the 25 dB bandwidth (i.e., the two-sided bandwidth define by frequencies beyond which the signal spectrum is always at least 25 dB below the spectrum peak) for X-band deep space missions. This recommendation is summarized in Fig. 1.

Table 1. Operating E_b/N_0 and E_s/N_0 values for Different Channel Codes

Code	E_b/N_0 (dB)	E_s/N_0 (dB)
(8920,1/6)	-0.092	-7.87
(8920,1/4)	0.19	-5.83
(8920,1/3)	0.45	-4.32
(8920,1/2)	1.07	-1.94
(LDPC,2/3)	2.02	0.26
(LDPC,4/5)	3.03	2.06
RS-(255,223)	6.51	5.93

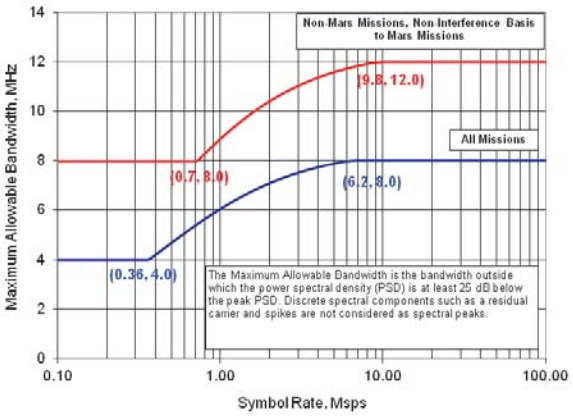

Figure 1. 25 dB Bandwidth Limit vs. Symbol Rate According to SFCG 23-1 Recommendation (Graph from SFCG 23-1 Recommendation Document)

Note that for coded channels, the information data rate limit is equal to the uncoded data rate limit times the code rate. Also note that the limits for BPSK are for an unfiltere signal. With filtering the BPSK could support higher data rates; however, since there are no standard filterin techniques for BPSK, we concentrate solely on the unfiltere case. Also note that the limits depicted in Tables 2 & 3 do not take into account things such as frame synchronization markers and additional channel symbols that turbo codes produce for each codeword when the encoding registers are cleared. However, for the analysis presented here, these are sufficientl accurate.

Receiver Structures and Carrier Tracking Loop Performance

As mentioned before, the receiver structures for GMSK are based on OQPSK receivers. In this paper we consider two such structures and discuss their performance based on the

[2]These values were calculated based on exponential curve fit for results obtained through simulations.

[3]Emails From Miles Sue of JPL's Spectrum Management Group

Table 2. Information Data Rate Limits Due to Spectrum Limitation, Mars Missions

Channel Code	BPSK, (Mbps)	GMSK (Mbps)
(8920,1/6)	0.060	1.03
(8920,1/4)	0.090	1.55
(8920,1/3)	0.120	2.07
(8920,1/2)	0.180	3.10
(LDPC,2/3)	0.240	4.13
(LDPC,4/5)	0.288	4.96
RS-(255,223)	0.315	5.42
Uncoded	0.36	6.20

Table 3. Information Data Rate Limits Due to Spectrum Limitation, non-Mars Missions

Channel Code	BPSK, (Mbps)	GMSK (Mbps)
(8920,1/6)	0.120	1.53
(8920,1/4)	0.180	2.30
(8920,1/3)	0.240	3.07
(8920,1/2)	0.360	4.60
(LDPC,2/3)	0.480	6.13
(LDPC,4/5)	0.576	7.36
RS-(255,223)	0.630	8.05
Uncoded	0.72	9.20

analysis done by Simon [3][4], Kinman[4], and Kinman and Berner [5].

The firs structure is a modificatio of the QPSK carrier tracking loop in which one of the quadrature channels is delayed by one binary symbol time,[5] T. The advantage of this method is that the structure is very simple and can leverage existing QPSK receiver structures with very little modifica tion (adding a binary symbol delay to one of the quadrature channels). The disadvantage of this structure is that it has substantial "squaring losses" in the carrier loop (more on this later). In addition, because the receiver structure essentially estimates four times the carrier phase, it could be subject to quarter-cycle slips. Therefore, the receiver requires a high loop SNR (LSNR) to maintain lock. As a result, for a given loop bandwidth, B_L, the required P_t/N_0 for the receiver to maintain lock is rather large. As we will show, this limits the utility of the receiver at lower data rates. The carrier tracking loop for this receiver is shown in Fig. 2. This structure is suboptimal in the maximum a posteriori (MAP) sense. However, because it is derived from a QPSK design (the QPSK carrier tracking loop is identical to the tracking loop in Fig. 2 but without the matched filter and the "T delay" block), from an implementation point of view is economical. This structure has been implemented in the BVR (without the matched filters for OQPSK tracking. It should be noted that the matched filter (MF blocks) are matched to $C_0(t)$, the firs constituent component of Laurent's decomposition of the pre-coded GMSK signal [4].[6] Use of this component with $BT = 0.5$ is proven to be almost as good as a truly optimized

[4]Technical Note, Kinman, P. "Radio Losses for Pre-Coded GMSK"

[5]For OQPSK receivers, this is typically noted as "$T_s/2$," half the channel symbol period. However, since we are dealing with GMSK which does not strictly have channel symbols, the use of binary symbol time "T" is more correct.

[6]Kinman, P., "Signal Structure and Power Spectral Density of Pre-Code GMSK," CSU Fresno Memorandum JPL-5, Januaray 11, 2006.

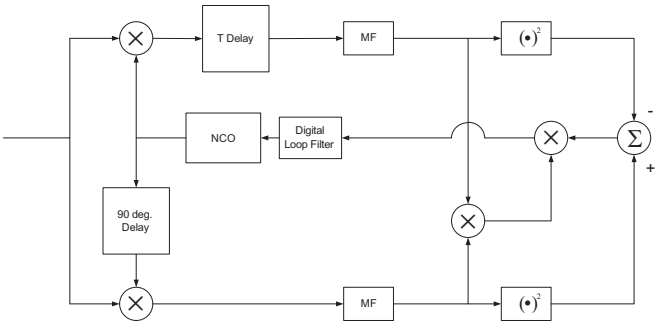

Figure 2. The "Suboptimum" GMSK Carrier Tracking Loop

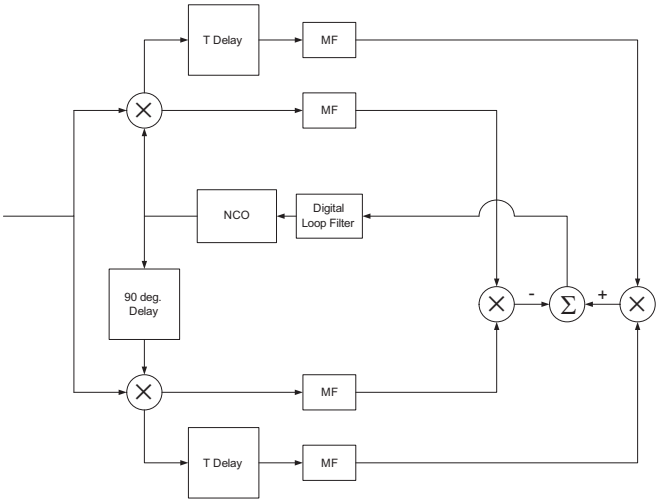

Figure 3. The "Optimum" GMSK Carrier Tracking Loop

receiver for GMSK and that the use of additional components of the Laurent's decomposition of the GMSK signal is not necessary [4]. It should also be noted that currently, the DSN supports GMSK tracking with BVR configure for OQPSK tracking, i.e., without the matched filter depicted in Fig. 2. As we will show this will produce some additional losses beyond the normal tracking losses due to the signal/receiver mismatch.

The second structure is based on a optimum MAP tracking loop for OQPSK (see Fig. 3). This figur represents the low SNR approximation of the OQPSK MAP tracking loop. It also requires knowledge of the symbol timing from the symbol tracking loop which is not depicted in this figur and not addressed in this paper. It should be noted that depending on how the symbol timing is obtained, this receiver could have significan losses beyond what is derived in this paper. As seen from Fig. 3, the tracking loop has a different structure and relies on four matched filter and two "T delay" blocks, but it does not have the two squaring elements of the structure in Fig. 2. As we will show, however, its performance is substantially better than the tracking loop in Fig. 2. Again the MF block are matched to $C_0(t)$, the firs component of the Laurent's decomposition of the GMSK signal.

Note that the tracking loops illustrated in Figs. 2 & 3 are more complex than that used for BPSK.

As shown in [3], the structure in Fig. 2 essentially tracks four times the carrier frequency. This produces a quarter-cycle ($\pi/2$) phase ambiguity in the reconstructed carrier. In

practice, this phase ambiguity is resolved by the telemetry frame synchronization process after the tracking loop is in lock. Once the ambiguity is resolved, it is highly desirable to prevent the tracking loop from having quarter-cycle slips as that would lead to loss of telemetry frame synchronization. Because of this, the phase error variance of the tracking has to be kept very small as to make the probability of quarter-cycle slips vanishingly small. Although we have not yet simulated the performance of this tracking loop with GMSK, we can use the results from the analysis of this tracking loop with OQPSK as an approximation for its performance with GMSK.

The tracking loop in Fig. 3 essentially tracks two times the carrier frequency and thus is subject to a half-cycle (π) phase ambiguity. Again this ambiguity is resolved through telemetry frame synchronization. Similarly, the loop has to have a relatively low phase error variance in order to make the probability of half-cycle slips vanishingly small.

For both tracking loops, the loop SNR which is the inverse of the tracking loop phase error variance is given by:

$$\rho = \sigma_{\phi}^{-2} = S_L \cdot \frac{P_t}{N_0} \cdot \frac{1}{B_L} \tag{2}$$

where S_L is the loop "squaring loss"[7]. For the tracking loop in Fig. 2, we assume that S_L is the same as that derived by Simon for OQPSK tracking [3] and is given by:

$$S_L\left(E_s/N_0\right) = \frac{1/4}{1 + \frac{9}{E_s/N_0} + \frac{3}{2(E_s/N_0)^2} + \frac{3}{16(E_s/N_0)^3}} \tag{3}$$

For the tracking loop in Fig. 3 the squaring loss was calculated by Kinman based on simulations he had performed. For a $BT = 0.5$, the squaring loss is given by:

$$S_L\left(E_s/N_0\right) = \frac{2}{3} \cdot \frac{2E_s/N_0}{1 + 2E_s/N_0} \tag{4}$$

It should be noted that for BPSK residual carrier signaling using PLL for carrier tracking, the loop SNR is given simply by:

$$\rho = \sigma_{\phi}^{-2} = \frac{P_c}{N_0} \cdot \frac{1}{B_L} \tag{5}$$

where P_c/N_0 is the carrier power to noise spectral density ratio.

As mentioned before, each of the tracking loops need to have a relatively low phase error variance (high loop SNR). Similarly the PLL used for tracking BPSK carrier needs to have a minimum loop SNR (maximum phase error variance) to achieve lock. In this paper, we assume that the minimum loop SNR for the carrier tracking loop in Fig. 2 is 25 dB, for the carrier tracking loop in Fig. 3 is 17 dB and for the PLL with residual carrier is 11 dB.

Radio Losses

Radio losses are define as the degradation in the performance of channel code relative to its baseband performance over an additive white Gaussian noise (AWGN) channel for a given frame error rate (FER) performance due to imperfect carrier tracking. In order to evaluate the radio losses of a channel we firs have to evaluate the performance of the link with imperfect carrier tracking. At high data rates, where the update rate of the carrier tracking loop is significantl lower than the channel symbol rate, the effective frame error rate of the channel is given by [6]:

$$F\left(\frac{E_b}{N_0}, \sigma_{\phi}\right) = \int_{\phi=-\pi}^{\phi=\pi} f_{FER}\left(E_b/N_0, \phi\right) p_{\Phi}\left(\phi, \sigma_{\phi}\right) d\phi \tag{6}$$

where E_b/N_0 is the unitless (not in dB) information bit signal-to-noise ratio; ϕ is the phase error; σ_{ϕ} is the phase error standard deviation; $p_{\Phi}\left(\phi, \sigma_{\phi}\right)$ is the phase error probability density function, and $f_{FER}\left(E_b/N_0, \phi\right)$ is the frame error rate as a function of the phase error and the bit signal-to-noise ratio.

For a given frame error rate, p, the radio loss is then define as

$$L_R\left(p, \sigma_{\phi}\right) = \frac{F^{-1}\left(p, \sigma_{\phi}\right)}{g_{FER}^{-1}(p)} \tag{7}$$

where $F^{-1}\left(p, \sigma_{\phi}\right)$ is the inverse of the function define in equation (6) such that

$$p = F\left(F^{-1}\left(p, \sigma_{\phi}\right), \sigma_{\phi}\right) \tag{8}$$

and $g_{FER}^{-1}(p)$ is the inverse of $g_{FER}(x)$, the code's frame error rate function for an additive white Gaussian noise (AWGN) channel with a bit SNR of x where x is unitless (not in dB).

For BPSK, $f_{FER}\left(E_b/N_0, \phi\right)$ is approximated by:

$$f_{FER}\left(x, \phi\right) = g_{FER}\left(\cos^2(\phi)x\right) \tag{9}$$

According to Kinman, $f_{FER}\left(E_b/N_0, \phi\right)$ for GMSK is approximated by:

$$f_{FER}(x, \phi) = g_{FER}\left(x \cdot r_c \cdot \frac{\cos^2(\phi)}{1 + 4x\left(R_1^2/R_0\right)\sin^2(\phi)}\right) \tag{10}$$

where R_1 and R_0 are parameters obtained from Laurent's decomposition of GMSK signal and r_c is the channel code rate. For the GMSK parameter $BT = 0.5$ that is recommended for deep-space applications, $R_0 = 0.99968$ and $R_1 = 0.41091$. Note that this approximation takes into account the intersymbol interference present in the GMSK signalling. Therefore, strictly speaking, when used in equation (6), the results reflec both the effects of intersymbol interference and imperfect carrier tracking. However, since the intersymbol interference losses for GMSK with $BT = 0.5$ are rather small, for the purposes of this discussion, all the losses calculated here are considered "radio losses."

The distribution $p_{\Phi}\left(\phi, \sigma_{\phi}\right)$ is a Tikhonov distribution. However, because each tracking loop estimates the carrier phase differently, the parameters and the range over which the distribution is define is different for each tracking loop.

For the residual carrier BPSK, the distribution is given by [6]:

$$p_{\Phi}\left(\phi, \sigma_{\phi}\right) = \frac{\exp\left(\cos(\phi)\sigma_{\phi}^{-2}\right)}{2\pi I_0\left(\sigma_{\phi}^{-2}\right)} \quad -\pi \leq \phi \leq \pi \tag{11}$$

[7]Even though the term S_L is referred to as the squaring loss, it is actually a power of 4 loss for the tracking loop depicted in Fig. 2. The term "squaring loss" is used to denote the loop performance degradation relative to a residual carrier tracking loop with the same signal power to noise ratio.

where I_0 is the zeroth order modifie Bessel function of the firs kind.

For the suboptimum tracking loop in Fig. 2 it is given by [3]:

$$p_\Phi(\phi,\sigma_\phi)=\begin{cases}\frac{\exp\left(\cos(4\phi)\sigma_\phi^{-2}/16\right)}{2\pi I_0\left(\sigma_\phi^{-2}/16\right)} & -\pi/4\le\phi\le\pi/4\\ 0 & \text{Otherwise}\end{cases} \tag{12}$$

Note that this distribution is define over a quarter cycle ($\pi/2$) range. This is because we assume that the loop operates at high SNR (>25 dB) and thus the probability of having a phase error outside of the quarter-cycle range is set to zero.

For the tracking loop in Fig. 3, $p_\Phi(\phi,\sigma_\phi)$ is given by:

$$p_\Phi(\phi,\sigma_\phi)=\begin{cases}\frac{\exp\left(\cos(2\phi)\sigma_\phi^{-2}/4\right)}{2\pi I_0\left(\sigma_\phi^{-2}/4\right)} & -\pi/2\le\phi\le\pi/2\\ 0 & \text{Otherwise}\end{cases} \tag{13}$$

Again here the range is limited to a half-cycle (π) because we assume that the loop operates with high enough SNR to avoid half-cycle slips.

Data Rate vs. P_t/N_0

Radio losses calculated from equations presented in the previous section can help evaluate supportable data rate for a given P_t/N_0 value. The process for evaluating the supportable data rate for a give channel and a given P_t/N_0 is slightly different for residual carrier BPSK than it is for GMSK.

For residual carrier BPSK, the transmitted power is divided between the carrier and the data channels. This division has to be done optimally so that the link can support the maximum data rate possible subject to a given f xed power budget. To put this formally, for a given frame error rate p, a carrier loop bandwidth B_L, a single-sided noise density, N_0 and a total received power of P_t, the following equation must be satisfie by data rate R_b and carrier power P_c:

$$\frac{P_t}{N_0}=\frac{P_c}{N_0}+g_{FER}^{-1}(p)\,L_R\left(p,\sqrt{\frac{N_0B_L}{P_c}}\right)R_b \tag{14}$$

Given equation (14) the maximum supportable data rate for a given value of total power-to-noise ration, P_t/N_0 is given by

$$R_b^{(max)}(P_t/N_0)=\max_{P_c/N_0}\frac{P_t/N_0-P_c/N_0}{g_{FER}^{-1}(p)\,L_R\left(p,\sqrt{\frac{N_0B_L}{P_c}}\right)} \tag{15}$$

Conversely, if the link needs to support a data rate R_b, then the minimum required P_t/N_0 is calculated by

$$\left(\frac{P_t}{N_0}\right)_{opt}=\min_{P_c/N_0}\frac{P_c}{N_0}+g_{FER}^{-1}(p)\,L_R\left(p,\sqrt{\frac{N_0B_L}{P_c}}\right)R_b \tag{16}$$

Equation (16) provides an insight into the behavior of the $(P_t/N_0)_{opt}$ as a function of the data rate R_b. At lower data rates, $(P_t/N_0)_{opt}$ is dominated by P_c/N_0 because of the minimum loop SNR requirement ($\rho_{threshold}$) for the carrier loop. Therefore, at lower data rates, we can lower P_c/N_0 because even with higher radio losses $(P_t/N_0)_{opt}$ would still be dominated by P_c/N_0. Given the loop SNR requirement, the minimum P_t/N_0 that the link needs to operate a residual carrier BPSK with carrier loop bandwidth of B_L is given by:

$$(P_t/N_0)_{\min}=\rho_{threshold}\cdot B_L \tag{17}$$

For a loop SNR requirement of 11 dB and a loop bandwidth of 3 Hz this translates into a minimum P_t/N_0 of 15.78 dB.

At higher data rates, P_t/N_0 is dominated by P_d/N_0, the data power-to-noise ratio. In equation (16) this is given by

$$\frac{P_d}{N_0}=g_{FER}^{-1}(p)\,L_R\left(p,\sqrt{\frac{N_0B_L}{P_c}}\right)R_b \tag{18}$$

As the data rate increases we want to minimize the radio losses, $L_R\left(p,\sqrt{\frac{N_0B_L}{P_c}}\right)$ in order to minimize P_t/N_0. Therefore, we put sufficien power into the carrier to reduce this value to near 0 dB (unity) with P_t/N_0 becoming

$$\frac{P_t}{N_0}\approx\ g_{FER}^{-1}(p)\,R_b\quad R_b>>0 \tag{19}$$

For GMSK, an equation similar to equation (18) is used to defin the relationship between R_b and P_t/N_0. However, this equation also depends on the code rate, r_c, of the channel code that is used since the squaring losses depend on E_s/N_0 value which in turn is determined by R_b, r_c and P_t/N_0:

$$\frac{E_s}{N_0}=\frac{P_t}{N_0}\cdot\frac{r_c}{R_b} \tag{20}$$

Using the relationship in equation (20) in conjunction with equations (2) through (4) and equation (7) we have:

$$\frac{P_t}{N_0}=R_bg_{FER}^{-1}(p)\,L_R\left(p,\sqrt{\frac{N_0B_L}{P_tS_L\left(\frac{P_t}{N_0}\cdot\frac{r_c}{R_b}\right)}}\right) \tag{21}$$

Note that equation (21) cannot be used to directly calculate either P_t/N_0 as a function of R_b or vice versa. Therefore, numerical techniques are used to evaluate one as a function of the other.

We now consider the performance of the link at high data rates and at low data rates. At high data rate, P_t/N_0 increases; therefore, the radio losses approach 0 dB (unity) and the relationship in equation (19) holds for GMSK as well.

At lower data rates the tracking loop has to have a loop SNR of $\rho_{threshold}$. This means that the relationship between data rate, R_b and the required P_t/N_0 is governed by

$$\rho_{threshold}=\frac{P_t}{N_0}\frac{S_L\left(\frac{P_t}{N_0}\cdot\frac{r_c}{R_b}\right)}{B_L} \tag{22}$$

At very low data rates, $\frac{P_t}{N_0}\cdot\frac{r_c}{R_b}\to\infty$; therefore, in the limit, the minimum required P_t/N_0 for the link is given by:

$$\left(\frac{P_t}{N_0}\right)_{\min}=\frac{\rho_{threshold}B_L}{S_L(\infty)} \tag{23}$$

For the tracking loop in Fig. 2, $S_L(\infty)=1/4$ and for the tracking loop in Fig. 3, $S_L(\infty)=2/3$.

The data rate at which the link switches from regime governed by the required minimum loop SNR to the regime governed by minimum required FER, $R_b^{(switch)}$, is determined

by satisfying equations (21) and (22) simultaneously:

$$R_b^{(switch)} = \frac{\rho_{threshold} B_L}{g_{FER}^{-1}(p) L_R\left(p, \rho_{threshold}^{-0.5}\right) S_L\left(g_{FER}^{-1}(p) L_R\left(p, \rho_{threshold}^{-0.5}\right) r_c\right)} \quad (24)$$

Equation (24) provides insight as to what receiver is needed for GMSK. Since we want power efficien y on the link, we do not want to use more power than absolutely necessary to lock the carrier tracking loop. That in turn would mean that we want to keep $R_b^{(switch)}$ as low as possible. According to equation (24), the receiver design can help us in two ways. First, the smaller $\rho_{threshold}$, the smaller is $R_b^{(switch)}$. Second, if S_L is large (i.e., the squaring loss is small), then $R_b^{(switch)}$ will be small. For the two tracking loops under consideration, the tracking loop in Fig. 3 has an advantage in both cases. As already stated, the threshold loop SNR for the loop in Fig. 3 is 17 dB vs. 25 dB for the loop in Fig. 2. More to the point, however, is the substantially lower squaring loss that the loop in Fig. 3 (the "optimum" loop) has. This is illustrated in Fig. 4.

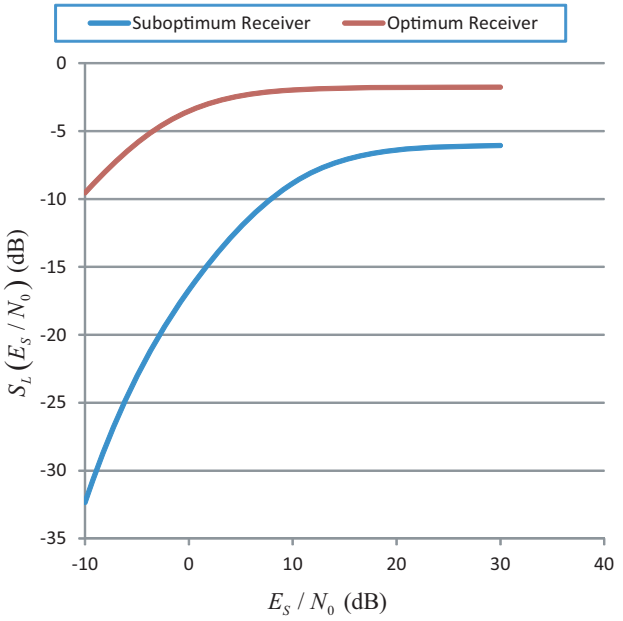

Figure 4. Squaring Losses for the "Optimum" and the "Suboptimum" Tracking Loops

As seen from this figure the squaring losses for the "suboptimum" loop are substantially higher than those for the "optimum" loop, with the loss at 0 dB E_S/N_0 being more than 13 dB greater.

Overall, for GMSK, for a given channel code and the given spectrum limitation, the supportable data rate vs. P_t/N_0 curves consist of three segments. This is illustrated in Fig. 5. The firs segment is when the P_t/N_0 is low. In this case, the data rate is adjusted so that the required loop SNR is maintained. Under this regime, the FER on the link is less than the minimum required FER. This regime continues until $R_b^{(switch)}$ where the second segment of the curve begins. The second segment of the curve is where the FER is equal to the minimum required FER. The loop SNR in this segment is greater than the minimum required loop SNR. The fina segment of the curve begins when the data rate becomes limited by the spectrum limits. In this segment, the data rate remains constant because of the spectrum limitations.

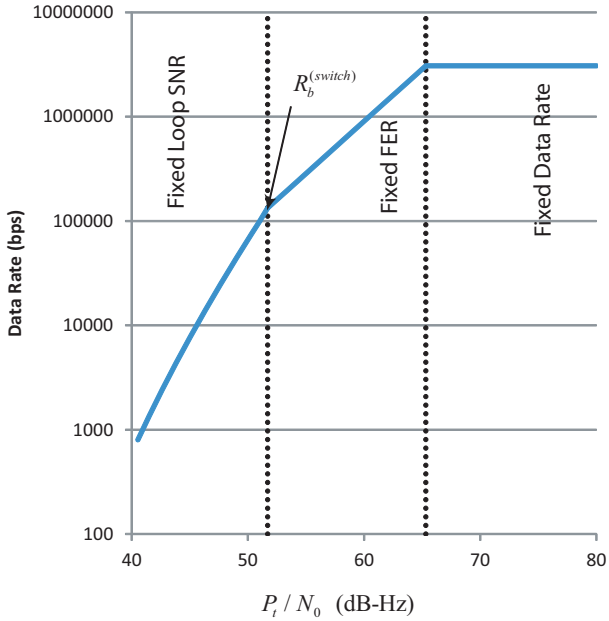

Figure 5. Supportable Data Rate vs. P_t/N_0 for non-Mars Missions, turbo code (8920,1/3), FER $\leq 10^{-4}$

Experimental Setup

As mentioned before, the current plan at the DSN to support GMSK using existing receivers configure for OQPSK demodulation. Since we do not have a theoretical model for the performance of GMSK with such a configuration it was decided to evaluate the performance of GMSK with different channel codes experimentally.

The setup for this experiment is shown in Fig. 6. As seen from this figure turbo encoded file generated off line are modulated onto the GMSK signal using a vector signal generator. White Gaussian noise is then added to this signal. The resulting signal is then fed to the DSN downlink telemetry and tracking receiver (a BVR plus the decoder) where the signal is decoded and demodulated. As part of the decoding and the demodulation process, the number of processed coded frames, the number of frames in error, carrier and symbol loop SNR values and E_s/N_0 are reported. These values are then used to calculate the FER and to evaluate the performance of the receiver.

Rate 1/6, 1/3 and 1/2 turbo codes were used with several different data rates. These are listed in Table 4. For each data rate for each code, initially a high value of E_s/N_0

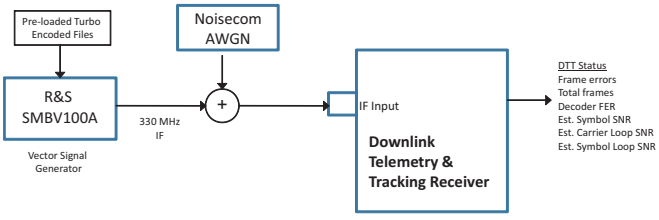

Figure 6. Experiment Setup for Evaluating Coded GMSK Performance with Existing DSN Receivers

Table 4. Experimental Data Rates for Different Turbo Codes

Code	Data Rates
(8920,1/2)	27 kbps 37 kbps
(8920,1/3)	50 kbps 75 kbps 125 kbps
(8920,1/6)	150 kbps 200 kbps

was used to lock up the receiver. After the receiver was locked up, E_s/N_0 was varied and the frame error rates were recorded. The frame error rates were then compared against the performance of the receivers with BPSK modulation and against the theory in order to evaluate the receiver losses.

Since we have assumed that the carrier tracking loop requires a minimum loop SNR, we wanted to verify this assumption experimentally. Determining the acquisition LSNR (the LSNR at which the receiver can acquire the signal) could be very time consuming (acquisition is inherently a probabilistic process and determining the acquisition LSNR requires many statistical trials); therefore, we decided only to verify whether or not the receiver can acquire with a nominal loop SNR of 25 dB (the minimum loop SNR assumed for the suboptimum GMSK receiver).

A carrier tracking loop bandwidth of 3 Hz was used in all cases.

3. RESULTS

Analytical Results

In this section, we present the analytical results that were obtained based on the discussion of data rate limits and radio losses in the previous section. The firs order of business is to evaluate the supportable data rate for each code with each modulation as a function of P_t/N_0 for Mars and non-Mars missions. In all cases a loop bandwidth of 3 Hz was assumed.

For BPSK, the results are shown in Figs. 7 & 8; for GMSK with the suboptimum receiver, the results are shown in Figs. 9 & 10, and for GMSK with the optimum receiver, the results are shown in Figs. 11 & 12. For comparison purposes, the upper envelopes for all cases considered are shown in Figs. 13 & 14 for Mars and non-Mars missions, respectively. Detailed descriptions of each envelope in terms of data rates, P_t/N_0 values and channels codes are given in Tables 6 through 11.

As seen from these figures over the range of data rates considered, for both BPSK and GMSK with the optimum receiver, the lower rate codes have a performance advantage over the higher rate codes until the data rate is limited by the spectrum. However, for GMSK with the suboptimum receiver at lower data rates, the higher rate codes outperform the lower rate codes. This is because the lower rate codes have higher squaring losses, thus they require larger P_t/N_0 values to meet the minimum loop SNR requirement.

In the important data rate range of 60 kbps to 1 Mbps which covers the data rate requirements for most of the Discovery class and the New Frontiers class missions, the optimum receiver structure depicted in Fig. 3 has a significan advantage

Table 5. $R_b^{(switch)}$ Values for Different Codes for GMSK with the Suboptimum Receiver

Code	$R_b^{(switch)}$ (bps)	P_t/N_0
(8920,1/6)	577,648	57.59
(8920,1/4)	237,174	54.01
(8920,1/3)	133,111	51.74
(8920,1/2)	55,067	48.57
(LDPC,2/3)	24,343	46.03
(LDPC,4/5)	12,589	44.21
RS-(223,255)	2,648	40.95

over the suboptimum receiver structure in Fig. 2. This is shown in Figs. 15 & 16. As seen from these figures over this critical range of data rates, because the optimum receiver allows the use of (8920,1/6) code, the optimum receiver requires much lower P_t/N_0 (by as much as 1.2 dB) to achieve the same data rate.

It should be note that with filtere BPSK, the BPSK curves will be able to support higher data rates for each codes. Therefore, it may be possible to use BPSK modulation with lower rate channel codes for data rates between 60 Kbps and 1 Mbps.

Experimental Results

The experimental results are shown in Figs. 17 through 19 and in Tables 12 & 13. As seen from these, because the BVR does not have matched filter for GMSK tracking, the link incurs substantial losses compared to the theoretical performance of the codes and the BPSK performance of the codes with the BVR. We calculated these losses for each data rate for each code for an FER of 10^{-4} by curve-fittin and extrapolating the experimental data. As seen in Table 12, the losses are greatest for the (8920,1/6) code ($>$ 1 dB) and smallest for the (8920,1/2). It should be noted that the reported LSNR by the receiver for (8920,1/6) code is lower than that reported for (8920,1/3) which in turn is lower than that reported for (8920,1/2) code. This indicates that some of the losses observed are not only due to the mismatch between the receiver structure and the signal but also due to poor carrier tracking by the receiver which in turn produces additional radio losses. This explains why the FER curve for 200 kbps data rate with (8920,1/6) exhibits lower losses than that for the 150 kbps data rate.

Note that in terms of absolute performance, (8920,1/3) code performs slightly better at 125 Kbps than the (8920,1/6) code at 150 Kbps because of the higher losses suffered by the (8920,1/6) code. This indicates again that a mission designer should take into account the ground receiver structure and its losses when planning the mission. Similarly, it indicates that the receiver design for the ground system should consider conditions under which the receiver might be used in terms of coding, symbol SNR and data rates.

We also tested to see whether or not the receiver can lock up with a LSNR of approximately 25 dB. In all cases (see Table 13), the receiver acquired the signal. It should be noted that while the receiver maintains lock for lower LSNR values, this does not guarantee that the receiver can lock up with these LSNR values. This indicates that the 25 dB minimum LSNR that was assumed in our analysis of the suboptimal receiver is perhaps too pessimistic.

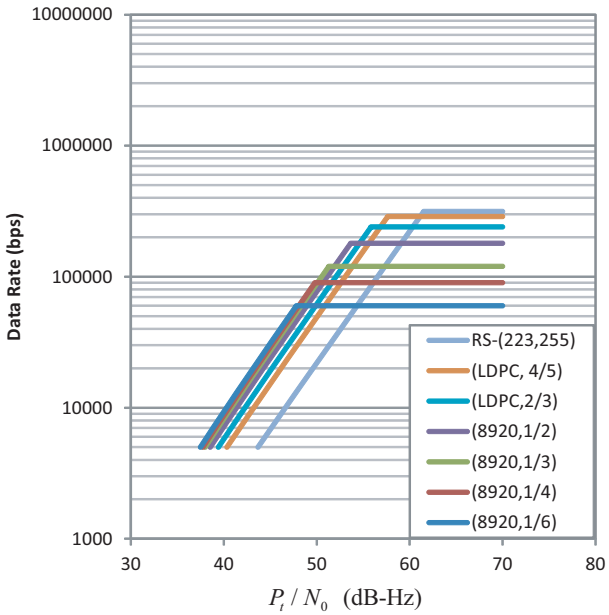

Figure 7. Data Rate vs. Required P_t/N_0 for Different Codes, Residual Carrier BPSK Modulation, Mars Missions

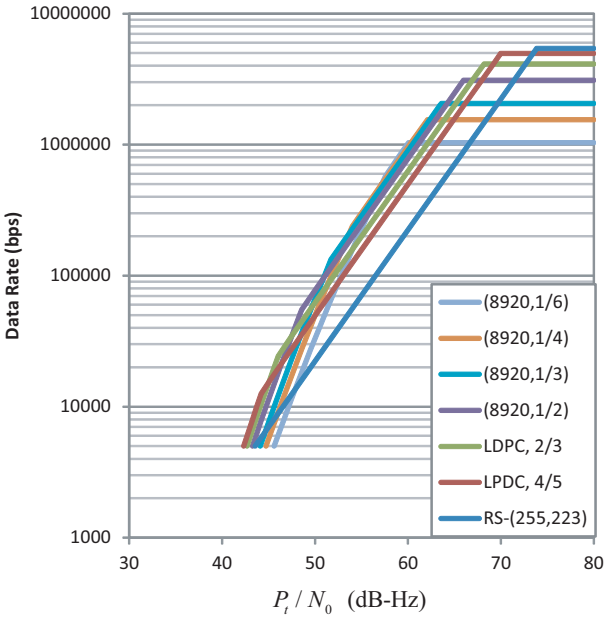

Figure 9. Data Rate vs. Required P_t/N_0 for Different Codes, GMSK Modulation with the Suboptimum Receiver, Mars Missions

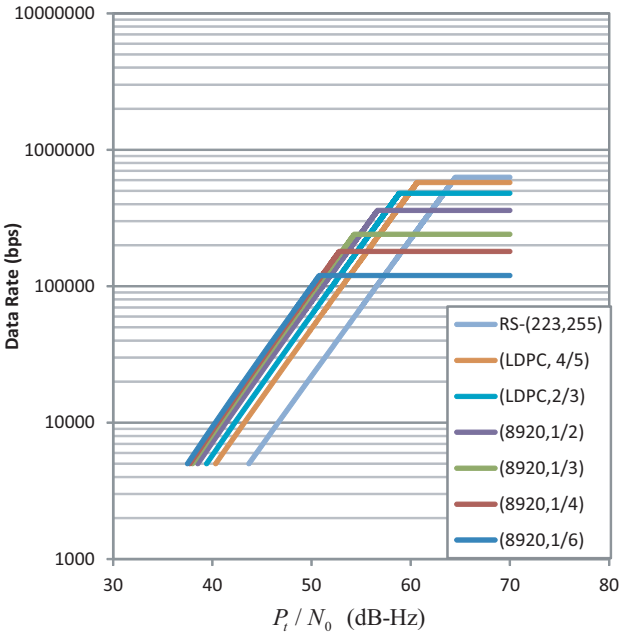

Figure 8. Data Rate vs. Required P_t/N_0 for Different Codes, Residual Carrier BPSK Modulation, non-Mars Missions

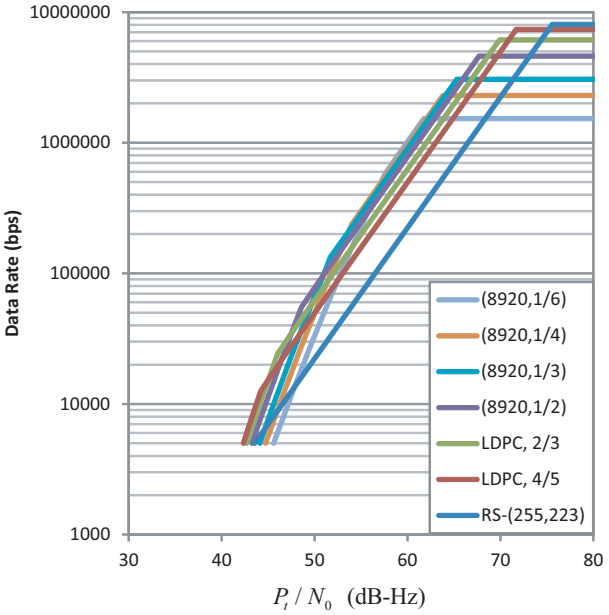

Figure 10. Data Rate vs. Required P_t/N_0 for Different Codes, GMSK Modulation with the Suboptimum Receiver, non-Mars Missions

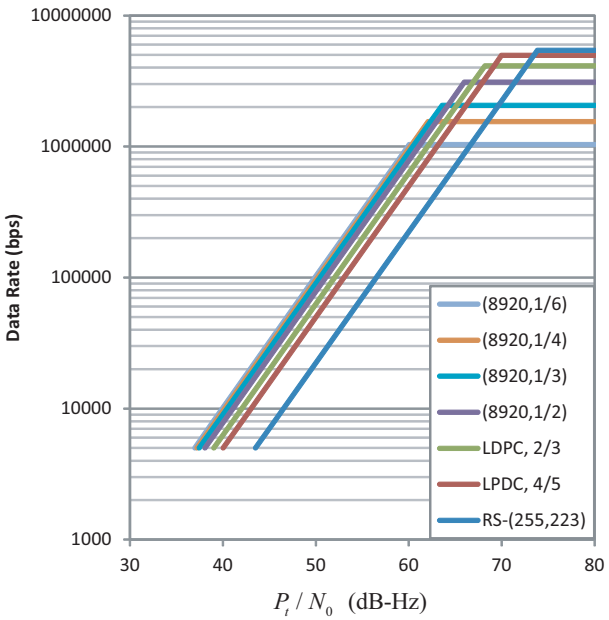

Figure 11. Data Rate vs. Required P_t/N_0 for Different Codes, GMSK Modulation with the Optimum Receiver, Mars Missions

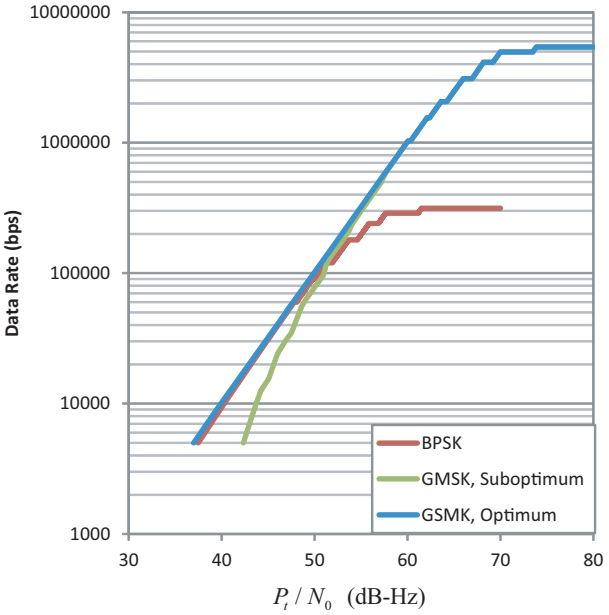

Figure 13. Data Rate Envelopes vs. Required P_t/N_0 for Residual Carrier BPSK, GMSK with the Suboptimum Receiver, and GMSK with the Optimum Receiver, Mars Missions

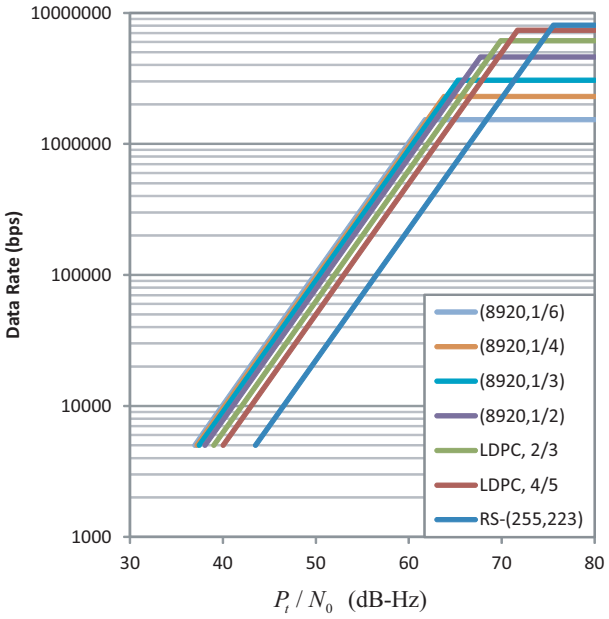

Figure 12. Data Rate vs. Required P_t/N_0 for Different Codes, GMSK Modulation with the Optimum Receiver, non-Mars Missions

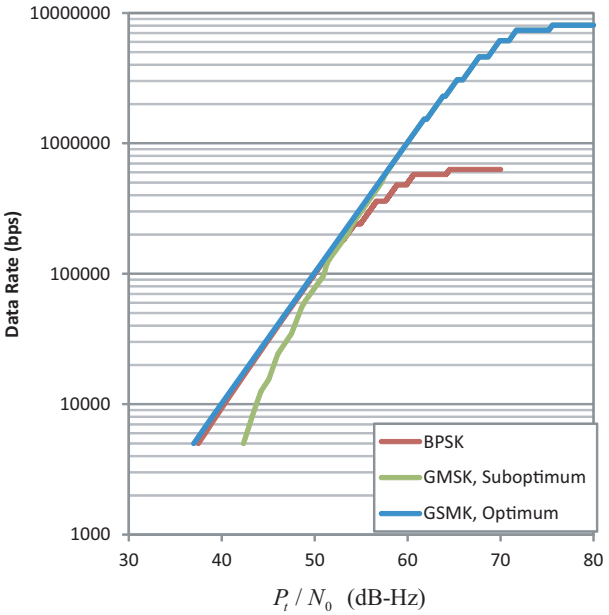

Figure 14. Data Rate Envelopes vs. Required P_t/N_0 Residual Carrier BPSK, GMSK with the Suboptimum Receiver, and GMSK with the Optimum Receiver, non-Mars Missions

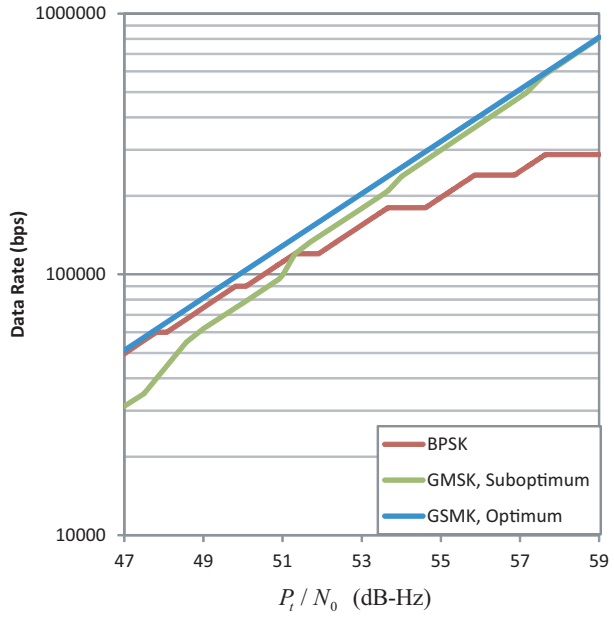

Figure 15. Data Rate Envelopes vs. Required P_t/N_0 for Residual Carrier BPSK, GMSK with the Suboptimum Receiver, and GMSK with the Optimum Receiver, Mars Missions, P_t/N_0 from 47 dB-Hz to 57 dB-Hz

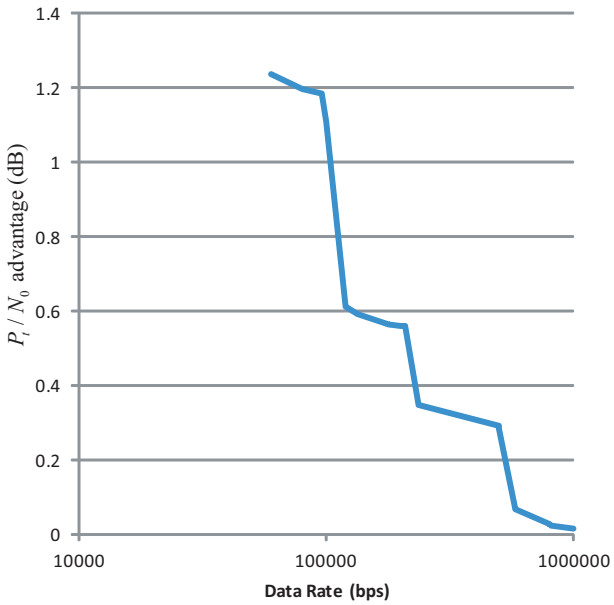

Figure 16. The Required P_t/N_0 Advantage of the Optimum Receiver over the Suboptimum Receiver for GMSK for Data Rates between 60 kbps to 1 Mbps

Table 6. P_t/N_0 and Data Rate Ranges for Residual Carrier BPSK, Mars Missions

P_t/N_0 Range (dB-Hz)	Data Rate Range (bps)	Channel Code
15.77 to 47.81	0 to 60,000	(8920,1/6)
47.81 to 48.07	60,000	(8920,1/6)
48.07 to 49.81	60,000 to 90,000	(8920,1/4)
49.81 to 50.07	90,000	(8920,1/4)
50.07 to 51.31	90,000 to 120,000	(8920,1/3)
51.31 to 51.91	120,000	(8920,1/3)
51.91 to 53.66	120,000 to 180,000	(8920,1/2)
53.66 to 54.61	180,000	(8920,1/2)
54.61 to 55.85	180,000 to 240,000	(LDPC,2/3)
55.85 to 56.85	240,000	(LDPC,2/3)
56.85 to 57.64	240,000 to 288,000	(LDPC,4/5)
57.64 to 61.13	288,000	(LDPC,4/5)
61.13 to 61.51	288,000 to 314,824	RS-(255,223)
$\geq$61.51	314,824	RS-(255,223)

Table 7. P_t/N_0 and Data Rate Ranges for Residual Carrier BPSK, non-Mars Missions

P_t/N_0 Range (dB-Hz)	Data Rate Range (bps)	Channel Code
15.77 to 50.78	0 to 120,000	(8920,1/6)
50.78 to 51.04	120,000	(8920,1/6)
51.04 to 52.79	120,000 to 180,000	(8920,1/4)
52.79 to 53.06	180,000	(8920,1/4)
53.06 to 54.30	180,000 to 240,000	(8920,1/3)
54.30 to 54.90	240,000	(8920,1/3)
54.90 to 56.66	240,000 to 360,000	(8920,1/2)
56.66 to 57.61	360,000	(8920,1/2)
57.61 to 58.85	360,000 to 480,000	(LDPC,2/3)
58.85 to 59.86	480,000	(LDPC,2/3)
59.86 to 60.65	480,000 to 576,000	(LDPC,4/5)
60.65 to 64.13	576,000	(LDPC,4/5)
64.13 to 64.52	576,000 to 629,647	RS-(255,223)
$\geq$ 64.52	629,647	RS-(255,223)

Table 8. P_t/N_0 and Data Rate Ranges for GMSK with the Suboptimum Receiver, Mars Missions

P_t/N_0 Range (dB-Hz)	Data Rate Range (bps)	Channel Code
42.33 to 45.05	5,000 to 15,539	(LDPC,4/5)
45.05 to 47.50	15,539 to 34,833	(LDPC,2/3)
47.50 to 50.92	34,833 to 96,127	(8920,1/2)
50.92 to 53.67	96,127 to 209,352	(8920,1/3)
53.67 to 57.16	209,352 to 497,109	(8920,1/4)
57.16 to 60.07	497,109 to 1,033,333	(8920,1/6)
60.07 to 60.33	1,033,333	(8920,1/6)
60.33 to 62.09	1,033,333 to 1,550,000	(8920,1/4)
62.09 to 62.35	1,550,000	(8920,1/4)
62.35 to 63.60	1,550,000 to 2,066,667	(8920,1/3)
63.60 to 64.22	2,066,667	(8920,1/3)
64.22 to 65.98	2,066,667 to 3,100,000	(8920,1/2)
65.98 to 66.94	3,100,000	(8920,1/2)
66.94 to 68.18	3,100,000 to 4,133,333	(LDPC,2/3)
68.18 to 69.19	4,133,333	(LDPC,2/3)
69.19 to 69.98	4,133,333 to 4,960,000	(LDPC,4/5)
69.98 to 73.47	4,960,000	(LDPC,4/5)
73.47 to 73.85	4,960,000 to 5,421,961	RS-(255,223)
$\geq$ 73.85	5,421,961	RS-(255,223)

Table 9. P_t/N_0 and Data Rate Ranges for GMSK with the Suboptimum Receiver, non-Mars Missions

P_t/N_0 Range (dB-Hz)	Data Rate Range (bps)	Channel Code
42.33 to 45.05	5,000 to 15,539	(LDPC,4/5)
45.05 to 47.50	15,539 to 34,833	(LDPC,2/3)
47.50 to 50.92	34,833 to 96,127	(8920,1/2)
50.92 to 53.67	96,127 to 209,352	(8920,1/3)
53.67 to 57.16	209,352 to 497,109	(8920,1/4)
57.16 to 61.77	497,109 to 1,533,333	(8920,1/6)
61.77 to 62.05	1,533,333	(8920,1/6)
62.05 to 63.81	1,533,333 to 2,300,000	(8920,1/4)
63.81 to 64.07	2,300,000	(8920,1/4)
64.07 to 65.31	2,300,000 to 3,066,667	(8920,1/3)
65.31 to 65.93	3,066,667	(8920,1/3)
65.93 to 67.70	3,066,667 to 4,600,000	(8920,1/2)
67.70 to 68.65	4,600,000	(8920,1/2)
68.65 to 69.90	4,600,000 to 6,133,333	LDPC, 2/3
69.90 to 70.90	6,133,333	LDPC, 2/3
70.90 to 71.70	6,133,333 to 7,360,000	LDPC, 4/5
71.70 to 75.18	7,360,000	LDPC, 4/5
75.18 to 75.57	7,360,000 to 8,045,490	RS-(255,223)
$\geq$ 75.57	8,045,490	RS-(255,223)

Table 10. P_t/N_0 and Data Rate Ranges for GMSK with the Optimum Receiver, Mars Missions

P_t/N_0 Range (dB-Hz)	Data Rate Range (bps)	Channel Code
36.98 to 60.05	5,000 to 1,033,333	(8920,1/6)
60.05 to 60.33	1,033,333	(8920,1/6)
60.33 to 62.09	1,033,333 to 1,550,000	(8920,1/4)
62.09 to 62.35	1,550,000	(8920,1/4)
62.35 to 63.60	1,550,000 to 2,066,667	(8920,1/3)
63.60 to 64.22	2,066,667	(8920,1/3)
64.22 to 65.98	2,066,667 to 3,100,000	(8920,1/2)
65.98 to 66.94	3,100,000	(8920,1/2)
66.94 to 68.18	3,100,000 to 4,133,333	(LDPC,2/3)
68.18 to 69.19	4,133,333	(LDPC,2/3)
69.19 to 69.98	4,133,333 to 4,960,000	(LDPC,4/5)
69.98 to 73.47	4,960,000	(LDPC,4/5)
73.47 to 73.85	4,960,000 to 5,421,961	RS-(255,223)
$\geq$ 73.85	5,421,961	RS-(255,223)

4. Conclusions and Caveats

In this paper we have shown that with proper receiver structure, GMSK modulation could be used at lower data rates with a performance nearly identical to that of residual carrier BPSK. However, with a supoptimum receiver, the GMSK utility would be greatly limited. This is especially important since only proper receiver structure allows for the use of lowest rate (8920,1/6) turbo code with GMSK modulation in the important data rate range of 60 kbps to 1 Mbps where the code cannot be used with residual carrier BPSK. In addition, we showed that DSN's BVR could be used to demodulate and decode precoded GMSK although with substantial losses.

It should be noted that most of the results presented in this paper are theoretical and are produced neither through experimentation nor simulation. This is especially true of the analysis of the tracking loop in Fig. 3 since it requires the knowledge of the symbol timing. Also note that the performance for BPSK is depicted for the unfiltere case only.

Table 11. P_t/N_0 and Data Rate Ranges for GMSK with the Optimum Receiver, non-Mars Missions

P_t/N_0 Range (dB-Hz)	Data Rate Range (bps)	Channel Code
36.98 to 61.76	5,000 to 1,533,333	(8920,1/6)
61.76 to 62.04	1,533,333	(8920,1/6)
62.04 to 63.80	1,533,333 to 2,300,000	(8920,1/4)
63.80 to 64.06	2,300,000	(8920,1/4)
64.06 to 65.31	2,300,000 to 3,066,667	(8920,1/3)
65.31 to 65.93	3,066,667	(8920,1/3)
65.93 to 67.70	3,066,667 to 4,600,000	(8920,1/2)
67.70 to 68.65	4,600,000	(8920,1/2)
68.65 to 69.90	4,600,000 to 6,133,333	LDPC, 2/3
69.90 to 70.90	6,133,333	LDPC, 2/3
70.90 to 71.70	6,133,333 to 7,360,000	LDPC, 4/5
71.70 to 75.18	7,360,000	LDPC, 4/5
75.18 to 75.57	7,360,000 to 8,045,490	RS-(255,223)
$\geq$ 75.57	8,045,490	RS-(255,223)

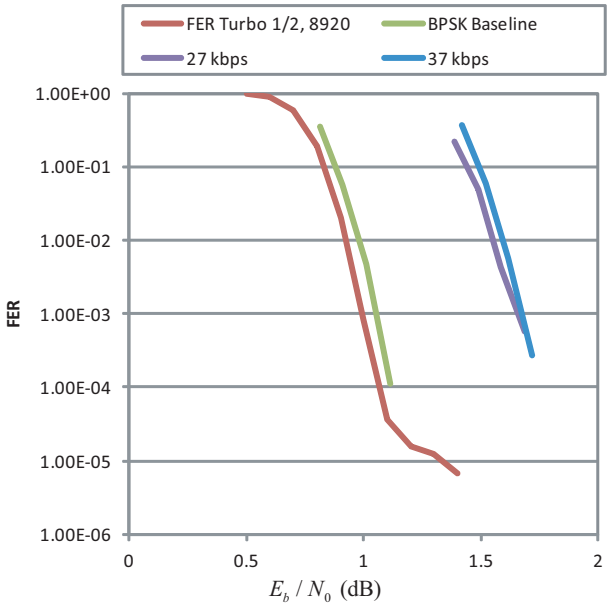

Figure 17. (8920,1/2) code FER vs. E_b/N_0, Theoretical, BPSK Baseline with the BVR, and GSMK with the BVR

Table 12. Measured GMSK E_b/N_0 and Losses Compared to BPSK Performance and Compared to Theoretical Performance, FER=10^{-4}

Code	Data Rates (kbps)	Calc. E_b/N_0 (dB)	Loss, BPSK	Loss Theory
(8920,1/2)	27	1.77	0.64	0.70
	37	1.77	0.64	0.70
(8920,1/3)	50	1.49	1.02	1.04
	75	1.45	0.98	1.00
	125	1.43	0.96	0.98
(8920,1/6)	150	1.46	1.61	1.74
	200	1.37	1.34	1.47

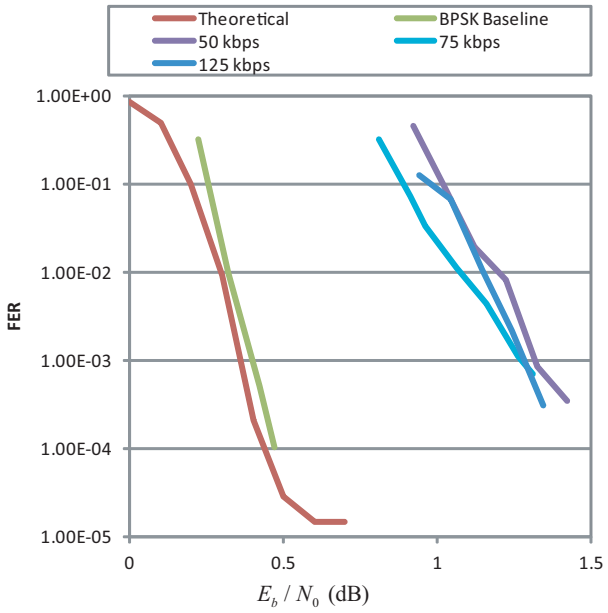

Figure 18. (8920,1/3) code FER vs. E_b/N_0, Theoretical, BPSK Baseline with the BVR, and GSMK with the BVR

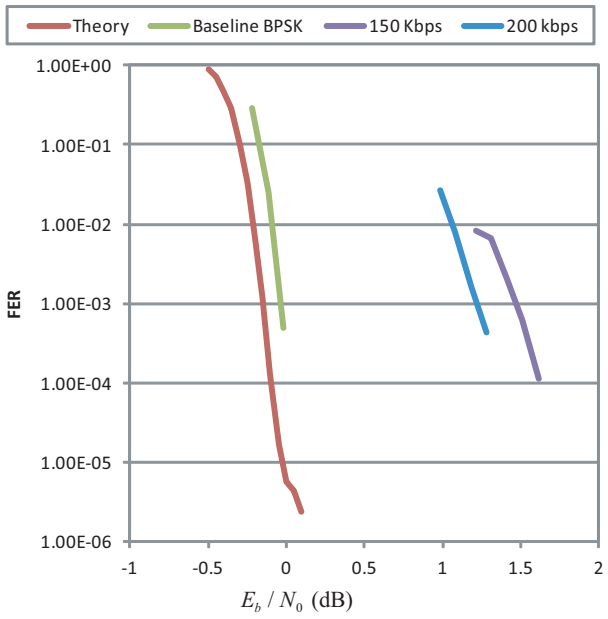

Figure 19. (8920,1/6) code FER vs. E_b/N_0, Theoretical, BPSK Baseline with the BVR, and GSMK with the BVR

Table 13. GMSK Acquisition Loop SNRs Tested with DSN BVR for Different Codes

Code	Data Rate (kbps)	Calc., LSNR (dB)	Meas. LSNR (dB)
(8920,1/2)	27	24.2	24.0
(8920,1/3)	75	25.7	25.0
(8920,1/6)	150	25.2	24.2

Therefore, the next step is to simulate the tracking loops in Figs. 2 & 3 with the different channel codes considered in this paper and evaluate the end to end performance of the link, including evaluation of the acquisition LSNR for each loop. In addition for Fig. 3 the simulation need to extend to the symbol tracking loop to evaluate the effects of imperfect symbol timing tracking on the carrier tracking loop. If these effects are substantial, the results presented in this paper could significantl change. We also need to extend the analysis for BPSK to the case of filtere BPSK. If the filtere BPSK can significantl increase the data rates with which lower rate codes could be used, the disadvantage of using the receiver in Fig. 2 may not appear as severe. As for the experimental results, further efforts should be made to evaluate the acquisition LSNR for the BVR for the GMSK signal.

ACKNOWLEDGMENTS

This work was performed at Jet Propulsion Laboratory, California Institute of Technology (Caltech), under a contract with National Aeronautics and Space Administration.

REFERENCES

[1] Moruta, K.; Hirade, K., "GMSK Modulation for Digital Mobile Radio Telephony," *IEEE Transaction on Communications*, Vol. 29, NO. 7, July 1981

[2] Laurent, P. A., "Exact and Approximate Construction of Digital Phase Modulations by Superposition of Amplitude Modulated Pulses (AMP)," *IEEE Transaction on Communications*, Vol. COM-34, NO. 2, February 1986

[3] Simon, M. K., "Carrier Synchronization of Offset Quadrature Phase-Shit Keying," *TMO Progress Report* 42-133, Pasadena, CA, May 15, 1998

[4] Simon, M. K., *Bandwidth-Efficien Digital Modulation with Application to Deep-Space Communications*, John Wiley & Sons, Hoboken, NJ, February 2003

[5] Kinman, P.W., and Berner, J.B.,"Carrier Tracking of Offset QPSK for Deep-Space Telemetry," *IEEE Aerospace Conference*, Big Sky, MT, March 2002

[6] Yuen, J. H ., ed., *Deep Space Telecommunications Systems Engineering,* Jet Propulsion Laboratory, California Institute of Technology, Pasadena, CA, 1982

BIOGRAPHY

Shervin Shambayati obtained his Bachelors of Science degree in Applied Mathematics and Engineering in 1989 from California State University, Northridge. Subsequently, he obtained his MSEE, Engineers Degree and Ph.D. from University of California, Los Angeles in 1991, 1993 and 2002, respectively. In 1993, Dr. Shambayati joined the Deep Space Communications Systems Group at Jet Propulsion Laboratory, California Institute of Technology, where he took part in development and testing of Deep Space Network's Galileo Telemetry receiver (DGT). In 1997, Dr. Shambayati joined the Information Processing Group at JPL, where he worked until 2009. With that group Dr. Shambayati has been involved in various

projects including Mars Global Surveyors Ka-Band Link Experiment II, Deep Space 1 Ka-band testing, 70m antenna Ka-band Task and the Mars Reconnaissance Orbiter Ka-band Demonstration for which he was the Principal Investigator. Currently, Dr. Shambayati is a member of Telecommunications Architecture group at JPL. His current research interests and activities include Ka-band link design, end-to-end system architecture studies for implementation of Ka-band and optical communications services in NASA's Deep Space Network, emergency mode communications for deep-space missions and programmatic support for Goldstone Solar System Radar.

Dennis K. Lee (S97 M98) earned his B.S. from Case Western Reserve University in 1997 and his M.S. from Rensselaer Polytechnic Institute in 1998, both in Electrical Engineering. Since 1999, he has been a member of technical staff in the Digital Signal Processing Research group at the Jet Propulsion Laboratory. Currently, his research interests include bandwidth efficien modulations and high rate signal processing.